

Molecular Imaging of Cancer Cells Using Plasmon-Resonant-Enhanced Third-Harmonic-Generation in Silver Nanoparticles**

By Shih-Peng Tai, Yana Wu, Dar-Bin Shieh, Lung-Jin Chen, Kuan-Jiuh Lin, Che-Hang Yu, Shi-Wei Chu, Chien-Huei Chang, Xuan-Yu Shi, Yu-Chieh Wen, Kung-Hsuan Lin, Tze-Ming Liu, and Chi-Kuang Sun*

Third-harmonic-generation (THG) has been emerged as an important noninvasive intravital imaging modality of *in vivo* biological research^[1–4] in recent years with the advantages including intrinsic optical sectioning capability due to the high-order nonlinearity nature and no energy release due to the virtual-state-transition characteristic,^[5–9] thus allowing much improved cell viability^[3,4] in contrast to current absorption-based fluorescence technologies. Although THG nonlinearity exists in all bio-materials, the Gouy phase shift effect substantially limits THG to be observed in the vicinity of interfaces where the first order or third order susceptibility discontinues.^[10] Therefore, THG is generally regarded as a morphological imaging tool due to its interface-sensitive nature, with limited capability for molecular imaging. It is thus highly desirable to develop exogenous THG contrast agents to trace the functions of a specific molecule, taking advantage of the noninvasive nature of the THG process. Recently, noble metal nanoparticles have been proved to be able to enhance various nonlinear optical signals through surface plasmon resonance.^[11–16] It should be ideal to adopt nanoparticles as molecular contrast agents of THG microscopy. However, these pre-

vious experiments proposed to enhance nonlinear emissions by matching excitation energy with the plasmon resonance energy of metal nanoparticles, which could induce strong laser absorption in nanoparticles while the induced temperature increase might alter the behaviors of the targeted bio-molecules or even induce thermal damages in the studied biological specimens.

In this letter, we demonstrate molecular THG microscopy by using silver nanoparticles as exogenous THG contrast agents. This demonstration was performed in cultured mouse bladder carcinoma cells (MBT2) and the matched cell line with knocked-down Her2/neu expression by RNAi. Through matching surface plasmon wavelength to THG wavelength, strong contrast can be provided by the silver nanoparticles under a THG microscope, while the laser wavelength is located in the biological penetration window and laser absorption in nanoparticles is also strongly reduced due to the huge spectral difference between the laser excitation wavelength and the plasmon resonance wavelength. By successfully conjugating anti-her2 antibodies with the citrated silver nanoparticles, Her2/neu in the cancerous cell membranes is successfully imaged with THG microscopy.

With the help of surface plasmon-resonance, nanometer-sized noble metals can serve as a nanoscopic optical resonant cavity. Metal nanoparticles with the plasmon resonance at the third harmonic of optical excitation, in the macroscopic point of view, is analogous to an optical third-harmonic oscillator.^[17,18] We chose silver nanoparticles for its blue-violet plasmon resonance wavelengths when soaked in water. For nonlinear biological *in vivo* imaging, near-infrared (NIR) femtosecond lasers are preferred as the THG excitation sources to increase the penetration depth and to reduce the potential optical damage. In particular, it has been demonstrated that the spectral transmission window of common biological tissues falls around 1200–1300 nm.^[3,4,19,20] With a 410-nm surface plasmon wavelength for THG resonance, the corresponding NIR laser wavelength is 1230 nm, which concurs with the biological transparency window. In contrast, gold nanoparticles are with a surface plasmon resonance wavelength of 520–560 nm and the corresponding laser wavelength of 1560–1680 nm^[21] could suffer strong water absorption, thus not suitable for *in vivo* biological imaging. Our recent spectral study of THG in silver nanoparticles, with a 410-nm plasmon wavelength,^[17] showed evident THG enhancement when the third-harmonic of the excitation matched the surface plasmon resonant frequency of silver nanoparticles, indicating that

[*] Prof. C.-K. Sun, Dr. S.-P. Tai, C.-H. Yu, Y.-C. Wen, Dr. K.-H. Lin, Dr. T.-M. Liu
Department of Electrical Engineering and Graduate Institute of Photonics and Optoelectronics
National Taiwan University
Taipei (Taiwan)
E-mail: sun@cc.ee.ntu.edu.tw

Y. Wu, Prof. D.-B. Shieh, C.-H. Chang, X.-Y. Shi
Institute of Oral Medicine and Center for Micro/Nano Science and Technology, and
Institute of Basic Medical Sciences
National Cheng Kung University
Tainan (Taiwan)

L.-J. Chen, Prof. K.-J. Lin
Department of Chemistry, National Chung Hsing University
Taichung (Taiwan)

Prof. S.-W. Chu
Department of Physics, National Taiwan University
Taipei, Taiwan

[**] We greatly thank the Prof. Ming-Derg Lai to kindly provide MBT2-KD cells. The authors also gratefully acknowledge financial support under the National Health Research Institute (NHRI-EX96-9201E1), National Science Council (NSC-95-2120-M-002-013, NSC-95-2314-B-006-067, and NSC-95-2120-M-002-004), Frontier Research of National Taiwan University, and National Taiwan University Research Center for Medical Excellence-Division of Genomic Medicine.

plasmon-enhanced silver nanoparticles could be an ideal contrast agent for THG microscopy.

To demonstrate molecule-specific THG microscopy by using silver nanoparticles as contrast agents, we synthesized silver nanoparticles conjugated with antibodies for the first time. The silver nanoparticles were first prepared by a citrate ion reduction method.^[22] A transmission electron microscope was used to imaging the particle size and shape. The measured average silver particle size is 30 nm (Ag-citrate) as shown in Figure 1a. The Ag-citrate nanoparticles were then modified with cysteamine to expose the amine group on the particles, and crosslinked to the antibody through EDC (1-Ethyl-3-[3-dimethylaminopropyl]carbodiimide) to form peptide bounds in between (Fig. 1c). Since the coating and size of the silver nanoparticles used for molecular imaging is different from that reported in our previous study^[17] (~ 6 nm with PVP coating), we also measured the surface plasmon resonant wavelength of silver nanoparticles soaked in water through their absorption spectra. Although the plasmon resonance peak of the 30-nm silver nanoparticle will be red-shifted relative to that of the 6-nm silver nanoparticle,^[23] the coating of nanoparticles also effects the surface plasmon resonant wavelength. As a result, the measured surface plasmon resonant wavelength of the 30-nm silver nanoparticles was found to be located at ~ 410 nm (Fig. 1b), ideal for THG imaging. Since the THG intensity nonlinearly increases with size when the nanoparticle is much smaller than the laser spot size,^[24] 30-nm Ag-citrate nanoparticles should provide even better THG contrast compared with smaller nanoparticles.

We added silver nanoparticles conjugated with anti-Her2 antibodies into the cultured mouse bladder carcinoma line (MBT2) for imaging of Her2 expression in cancer cells. The Her2 molecule is one of the transmembrane receptor proteins for epidermal growth factors, and plays a key role in cell growth and anti-apoptotic signaling.^[25–27] The Her2 molecule is also important in cancer development, clinical prognosis, and therapeutic applications.^[28–30] Overexpression of Her2/neu in cancer lesion is a predictor for unfavorable clinical outcome with more aggressive growth behavior as well as resistance to some chemotherapy agents.^[28,29] On the other hand, the chemotherapeutic agent Herceptin, which is an antibody peptide drug, is only effective for Her2/neu highly expressed tumor cells.^[31] The MBT2 cell line is known to highly express Her2 molecules. As a control for the gene-expression-specific molecular imaging, we have transfected expression vector carrying RNAi against Her2/neu into the MBT2 cells and screened for the stable clone as the control group cancer cells. Western blot analysis revealed the Her2/neu knocked-down cancer cell line, MBT2-KD, expressed only about 15 % the level of the wild type line, as shown in Figure 2a. To demonstrate molecular imaging of cancer cells, we used a home-built THG microscope based on a femtosecond Cr:forsterite laser with an emission wavelength of 1230 nm,^[3,4] to match the THG wavelength with the silver plasmon resonance. Figure 2b–d show the epi-THG images of the wild type MBT2 cells without and with the silver nanoparticle labeling, and MBT2-KD cells with silver nanoparticle labeling. By comparing these THG images, bright spots on the wild type

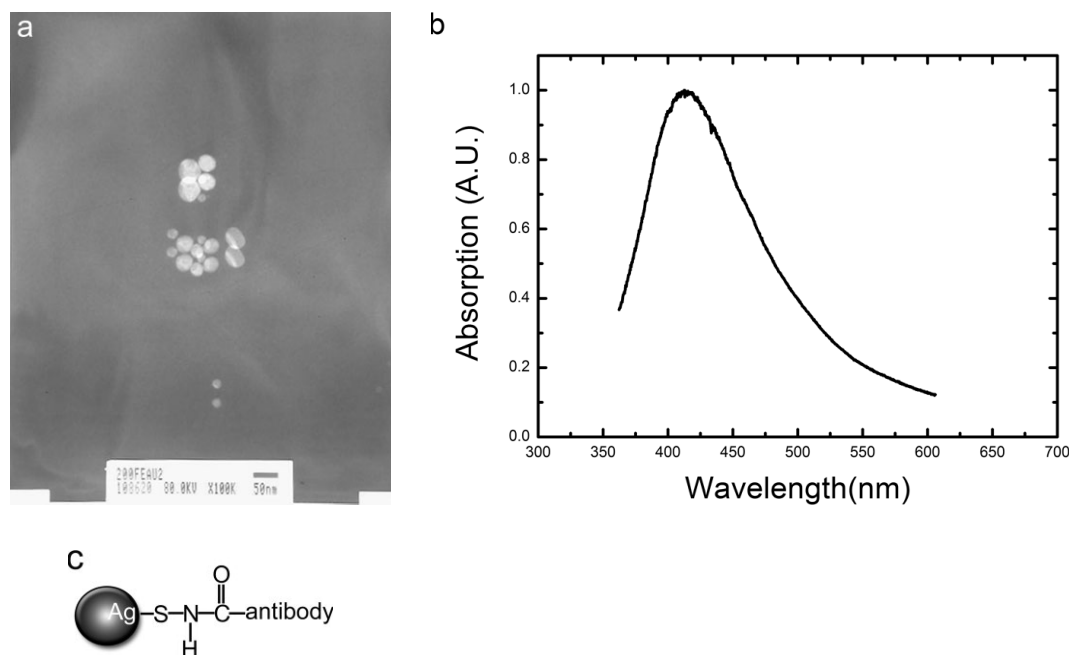


Figure 1. Characteristics of silver nanoparticles made by a citrate-ion reduction method. a) Transmission electron micrograph of silver nanoparticles used as the THG contrast agents of Her2 molecules. The measured average size of the particles is 30 nm in diameter. Scale bar: 50 nm. b) The absorption spectrum of the adopted silver nanoparticles soaked in water, with a resonant absorption peak at ~ 410 nm. c) The chemical schematic of the anti-antibody-conjugated silver nanoparticle.

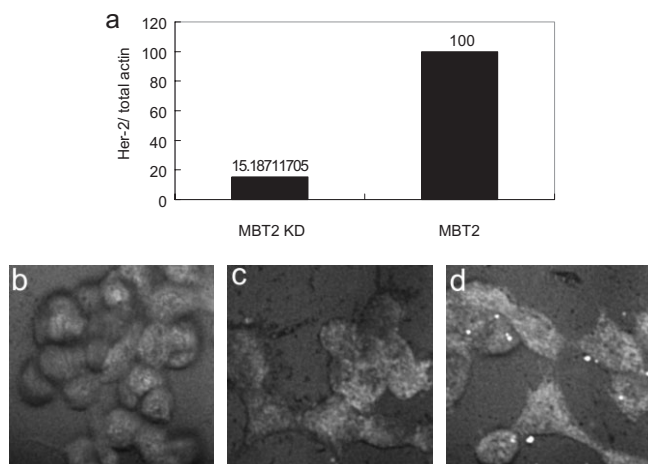


Figure 2. Demonstration of molecule-specific THG imaging of cancer cells. a) Densitometry quantification of Her-2 expression levels in the corresponding cancer cell lines from the autoradiograph of Western blot. b) THG image of wild type MBT2 cells without being treated with silver nanoparticles. c) THG image of Her2-knocked-down MBT2 cells treated with anti-Her2 antibody conjugated silver nanoparticles. d) THG image of wild type MBT2 cells treated with anti-Her2 antibody conjugated silver nanoparticles. Image size: $80\ \mu\text{m} \times 80\ \mu\text{m}$. All displayed epi-THG images are the superimposition of twenty horizontal sections. Silver nanoparticles significantly enhanced the THG signal intensity proportional to the endogenous Her-2 expression levels of the cancer cells.

cancer cell cytoplasmic membranes can be clearly observed (Fig. 2d), in sharp contrast to the MBT2-KD line (Fig. 2c) and in proportion to their endogenous Her-2 expression levels (Fig. 2a). This should be attributed to the THG signals from silver nanoparticles conjugated with anti-Her2 antibody. Molecule-specific THG microscopy is thus successfully demonstrated by using antibody-conjugated silver nanoparticles as exogenous THG contrast agents.

With a 410-nm plasmon resonance THG wavelength in water-based silver nanoparticles, the corresponding laser wavelength is 1230 nm, which is most penetrative and least damage for the biological specimens, while nanoparticle absorption is also minimized by moving the excitation wavelength far away from the plasmon resonance wavelength, with a huge 820-nm wavelength difference (2eV energy difference) never achieved before. In Figure 2d, epi-THG signals from the silver nanoparticles can be found to be orders of magnitude higher than the cell-induced epi-THG background signals, not just due to the strong plasmon effect, but also due to the nano-size effect of the silver particles. It is known that efficient direct backward-emitted THG can only be generated in a very thin (sub-micron) layer compared with the pump laser wavelength under tightly focused excitation fields.^[4,8,32–34] In order to outline the cell distribution in Figure 2d, the epi-THG signals from the silver nanoparticles were found to be saturated after adjusting the THG image contrast. Without saturation, the imaged spot size of the silver nanoparticle can be found to be $\sim 308\ \text{nm}$. This number is equal to the convolution value (309 nm) of the theoretical system resolution and a

30-nm nanoparticle size, and is slightly smaller than the convolution value (314 nm) of the theoretical system resolution and a 60-nm nanoparticle size. It is also well known that aggregation of silver nanoparticles will not only red-shift the plasmon wavelength but also reduce the surface plasmon density,^[23,35] thus reducing the THG efficiency under 1230-nm excitation. The strong epi-THG contrast should thus be contributed from a single nanoparticle. With a virtual transition characteristic, the silver-nanoparticle-induced THG signals do not suffer photobleaching^[36,37] and blinking^[38–41] problems, and are ideal for future long-term observations, after reduction of nano-toxicity with proper surface treatment. With accurate control of particle size, plasmon wavelength could be manipulated with a much narrower spectral width.^[23] With different excitation laser wavelengths or with a broad-band excitation light, multiple-color THG microscopy, aiming to image different molecules, should also be possible. Other nanoparticles with a strong plasmon resonance in the blue-violet wavelength should also be ideal for *in vivo* molecular THG imaging.

Experimental

The detailed synthesis of anti-body conjugated silver nanoparticles is described as follows. The Ag-citrate nanoparticles were centrifuged in 6000 rpm for 10 minutes to remove extra supernatant. The concentrated nanoparticles were added into $1\ \mu\text{M}$ cyteamine and 10 mM phosphate buffer (PB) (pH = 7) in original stock concentration for 4 hours and then washed twice to remove extra cysteamine. Then $10\ \mu\text{g}\ \text{ml}^{-1}$ anti-Her2 antibodies produced by hybridoma (MAb 4D5) were then added to PB (pH = 7) buffered cysteamine modified silver nanoparticles. The nanoparticles and antibodies mixture was then add $1\ \text{mg}\ \text{ml}^{-1}$ 1-Ethyl-3-[3-dimethylaminopropyl]carbodiimide (EDC) as a cross-linker reagent, and the whole reaction was stirred in $4\ ^\circ\text{C}$ for 4 hours. The anti-her2 modified nanoparticles were then washed by PB (pH = 7) for three times and added 0.05 % sodium azide as preservative and then stored in $4\ ^\circ\text{C}$ refrigerator.

The MBT2 and the MBT2-KD cells were cultured on chamber slides and fixed by 4 % paraformaldehyde. The cells were then blocked by 5 % milk, then exposed to the anti-Her2 conjugated silver nanoparticles ($0.2\ \text{ml}$ with $1.67\ \mu\text{M}$ concentration) for 1 hour and washed 3 times by phosphate buffered saline (PBS). The cells were then mounted on a slide with PBS.

The study of THG microscopy by using antibody conjugated silver nanoparticles as THG contrast agents was performed using a home-built femtosecond Cr:forsterite laser centered at 1230 nm with a 130-fs pulsewidth and a 110 MHz repetition rate [8]. The spectral full width half maximum of the laser output was about 20 nm. The infrared laser beam was first shaped by a telescope and then directed into a modified beam scanning system and an Olympus upright microscope. An IR water-immersion objective (Olympus UplanApo/IR 60X/NA 1.2) was used to focus laser beam into the observed specimens. The observed specimens were mounted on a stage with an axial resolution of 25 nm. The generated THG was collected by a NA 1.4 achromatic oil immersion condenser, and then directed into the PMT with a 410-nm narrow band interference filter in front. Details about our epi-THG microscope can be found in Ref. [8]. To ensure the signal we detected is THG, a spectrometer was used to confirm the detected THG wavelength before imaging. A power dependent study confirmed the cubic dependency of the detected THG signals.

Received: September 27, 2007

Revised: June 8, 2007

- [1] D. Yelin, Y. Silberberg, *Opt. Express* **1999**, *5*, 169.
- [2] L. Canioni, S. Rivet, L. Sarger, R. Barille, P. Vacher, P. Voisin, *Opt. Lett.* **2001**, *26*, 515.
- [3] C.-K. Sun, S.-W. Chu, S.-Y. Chen, T.-H. Tsai, T.-M. Liu, C.-Y. Lin, H.-J. Tsai, *J. Struct. Biol.* **2004**, *147*, 19.
- [4] S.-P. Tai, W.-J. Lee, D.-B. Shieh, P.-C. Wu, H.-Y. Huang, C.-H. Yu, C.-K. Sun, *Opt. Express* **2006**, *14*, 6178.
- [5] S.-W. Chu, I.-S. Chen, T.-M. Liu, C.-K. Sun, S.-P. Lee, B.-L. Lin, P.-C. Cheng, M.-X. Kuo, D.-J. Lin, H.-L. Liu, *J. Microsc.* **2002**, *208*, 190.
- [6] C.-K. Sun, C.-C. Chen, S.-W. Chu, T.-H. Tsai, Y.-C. Chen, B.-L. Lin, *Opt. Lett.* **2003**, *28*, 2488.
- [7] V. Barzda, C. Greenhalgh, J. A. der Au, S. Elmore, J. HGM van Beek, J. Squier, *Opt. Express* **2005**, *13*, 8263.
- [8] S.-P. Tai, T.-H. Tsai, W.-J. Lee, D.-B. Shieh, Y.-H. Liao, H.-Y. Huang, K. Y.-J. Zhang, H.-L. Liu, C.-K. Sun, *Opt. Express* **2005**, *13*, 8231.
- [9] D. Debarre, W. Supatto, A.-M. Pena, A. Fabre, T. Tordjmann, L. Combettes, M.-C. Schanne-Klein, E. Beaurepaire, *Nat. Methods* **2006**, *3*, 47.
- [10] J. M. Schins, T. Schrama, J. Squier, G. J. Brakenhoff, M. Müller, *J. Opt. Soc. Am. B* **2002**, *19*, 1627.
- [11] S. Nie, S. R. Emory, *Science* **1997**, *275*, 1102.
- [12] K. Kneipp, H. Kneipp, I. Itzkan, R. R. Dasari, M. S. Feld, *Chem. Rev.* **1999**, *99*, 2957.
- [13] H. Kano, S. Kawata, *Opt. Lett.* **1996**, *21*, 1848.
- [14] A. Podlipensky, J. Lange, G. Seifert, H. Graener, I. Cravetchi, *Opt. Lett.* **2003**, *28*, 716.
- [15] B. Lamprecht, J. R. Krenn, A. Leitner, F. R. Aussenegg, *Phys. Rev. Lett.* **1999**, *83*, 4421.
- [16] D. Yelin, D. Oron, S. Thiberge, E. Moses, Y. Silberberg, *Opt. Express* **2003**, *11*, 1385.
- [17] T.-M. Liu, S.-P. Tai, C.-H. Yu, Y.-C. Wen, S.-W. Chu, L.-J. Chen, M.-R. Prasad, K.-H. Lin, C.-K. Sun, *Appl. Phys. Lett.* **2006**, *89*, 043122.
- [18] E. M. Kim, S. S. Elovikov, T. V. Murzina, A. A. Nikulin, O. A. Aktipetrov, *Phys. Rev. Lett.* **2005**, *95*, 227402.
- [19] B. E. Bouma, G. J. Tearney, I. P. Bilinsky, B. Golubovic, J. G. Fujimoto, *Opt. Lett.* **1996**, *21*, 1839.
- [20] S.-W. Chu, I.-H. Chen, T.-M. Liu, P.-C. Chen, C.-K. Sun, B.-L. Lin, *Opt. Lett.* **2001**, *26*, 1909.
- [21] M. Lippitz, M. A. V. Dijk, M. Orrit, *Nano Lett.* **2005**, *5*, 799.
- [22] Z. S. Pillai, P. V. Kamat, *J. Phys. Chem. B* **2004**, *108*, 945.
- [23] U. Kreibig, M. Vollmer, *Optical Properties of Metal Clusters*, Springer Series in Material Science, Vol. 25, Springer, Berlin **1995**.
- [24] S. V. Popruzhenko, D. F. Zaretsky, W. Becker, *J. Phys. B* **2006**, *39*, 4933.
- [25] M. Campiglio, A. Locatelli, C. Olgiati, N. Normanno, G. Somenzi, L. Vigano, M. Fumagalli, S. Menard, L. Gianni, *J. Cell. Physiol.* **2004**, *198*, 259.
- [26] T. Faltus, J. Yuan, B. Zimmer, A. Kramer, S. Loibl, M. Kaufmann, K. Strebhardt, *Neoplasia* **2004**, *6*, 786.
- [27] W. Xia, J. Bisi, J. Strum, L. Liu, K. Carrick, K. M. Graham, A. L. Treece, M. A. Hardwicke, M. Dush, Q. Liao, R. E. Westlund, S. Zhao, S. Bacus, N. L. Spector, *Cancer Res.* **2006**, *66*, 1640.
- [28] O. Thuerigen, A. Schneeweiss, G. Toedt, P. Warnat, M. Hahn, H. Kramer, B. Brors, C. Rudlowski, A. Benner, F. Schuetz, B. Tews, R. Eils, H. P. Sinn, C. Sohn, P. Lichter, *J. Clin. Oncol.* **2006**, *24*, 1839.
- [29] K. I. Pritchard, L. E. Shepherd, F. P. O'Malley, I. L. Andrusis, D. Tu, V. H. Bramwell, M. N. Levine, *N. Engl. J. Med.* **2006**, *354*, 2103.
- [30] D. R. Emlet, R. Schwartz, K. A. Brown, A. A. Pollice, C. A. Smith, S. E. Shackney, *Br. J. Cancer* **2006**, *94*, 1144.
- [31] G. L. Plosker, S. J. Keam, *Drugs* **2006**, *66*, 449.
- [32] A. Volkmer, J. X. Cheng, X. S. Xie, *Phys. Rev. Lett.* **2001**, *87*, 023901.
- [33] J. X. Cheng, X. S. Xie, *J. Opt. Soc. Am. B* **2002**, *19*, 1604.
- [34] S.-Y. Chen, presented at the Conf. on Laser and Electro-optics/Quantum Electronics and Laser Science Conf. 2005 (CLEO/QELS 2005), Baltimore, MD, USA, May 22–27, 2005.
- [35] J. Zhang, J. R. Lakowicz, *J. Phys. Chem. B* **2005**, *109*, 8701.
- [36] S. M. Potter, C. M. Wang, P. A. Garrity, S. E. Fraser, *Gene* **1996**, *173*, 25.
- [37] S. K. Davis, C. J. Bardeen, *Photochem. Photobiol.* **2005**, *81*, 548.
- [38] M. Nirmal, B. O. Dabbousi, M. G. Bawendi, J. J. Macklin, J. K. Trautman, T. D. Harris, L. E. Brus, *Nature* **1996**, *383*, 802.
- [39] R. G. Neuhauser, K. T. Shimizu, W. K. Woo, S. A. Empedocles, M. G. Bawendi, *Phys. Rev. Lett.* **2000**, *85*, 3301.
- [40] M. Kuno, D. P. Fromm, H. F. Hamann, A. Gallagher, D. J. Nesbitt, *J. Chem. Phys.* **2000**, *112*, 3117.
- [41] B. Lounis, H. A. Bechtel, D. Gerion, P. Alivisatos, W. E. Moerner, *Chem. Phys. Lett.* **2000**, *329*, 399.